Biochemical and Biophysical Research Communications **291,** 1–7 (2002)
doi:10.1006/bbrc.2002.6391, available online at http://www.idealibrary.com on IDEAL®

Cyanide Binding to cd_1 Nitrite Reductase from *Pseudomonas aeruginosa*: Role of the Active-Site His369 in Ligand Stabilization

Wenliang Sun,*[,1] Marzia Arese,*[,1] Maurizio Brunori,* Didier Nurizzo,† Kieron Brown,† Christian Cambillau,† Mariella Tegoni,† and Francesca Cutruzzolà*[,2]

**Dipartimento di Scienze Biochimiche "A. Rossi Fanelli" and Centro di Biologia Molecolare del CNR, Università di Roma "La Sapienza," Rome, Italy; and †Architecture et Fonction des Macromolécules Biologiques, UMR 6098–CNRS and Universités de Marseille I & II, 13402 Marseille Cedex 20, France*

Received December 23, 2001

Cyanide binding to fully reduced *Pseudomonas aeruginosa* cd_1 nitrite reductase (*Pa* cd_1 NiR) has been investigated for the wild-type enzyme and a site-directed mutant in which the active-site His369 was replaced by Ala. This mutation reduces the affinity toward cyanide (by ~13-fold) and especially decreases the rate of binding of cyanide to the reduced d_1 heme (by ~100-fold). The crystal structure of wild-type reduced *Pa* cd_1 NiR saturated with cyanide was determined to a resolution of 2.7 Å. Cyanide binds to the iron of the d_1 heme, with an Fe-C-N angle of 168° for both subunits of the dimer and only His369 is within hydrogen bonding distance of the nitrogen atom of the ligand. These results suggest that in *Pa* cd_1 NiR the invariant distal residue His369 plays a dominant role in controlling the binding of anionic ligands and allow the discussion of the mechanism of cyanide binding to the wild-type enzyme. © 2002 Elsevier Science (USA)

***Key Words: Pseudomonas aeruginosa;* cd_1 nitrite reductase; cyanide binding; site-directed mutagenesis; heme protein.**

In *Pseudomonas aeruginosa*, the conversion of nitrite to nitric oxide in the denitrification pathway is catalyzed by nitrite reductase, a periplasmic homodimer of two 60-kDa subunits (1, 2). Each monomer contains both a covalently bound c heme and a noncovalently bound d_1 heme. Extensive spectroscopic and functional evidence has shown that the c heme is the site of electron entry from donor proteins (e.g., azurin and cytochrome c_{551}), whereas the d_1 heme is the site of NO_2^- binding and catalysis (3). The enzyme catalyzes not only the one-electron reduction of NO_2^- to NO, but also the four-electron reduction of dioxygen to water, albeit with a much lower efficiency (4, 5); only the former reaction was demonstrated to occur *in vivo*.

The three-dimensional structure of *Pseudomonas aeruginosa* cd_1 nitrite reductase (*Pa* cd_1 NiR) has been solved by crystallography in different redox states (6–8). Each subunit consists of an N-terminal α-helical domain containing the c heme and a C-terminal eight-bladed β-propeller domain embracing the d_1 heme. A striking phenomenon observed in oxidized *Pa* cd_1 NiR is the "domain swapping" of the N-terminal region, which brings Tyr10 of one monomer in the d_1 heme active site of the other (6). Besides Tyr10, the distal side of the d_1 heme pocket is composed of other important amino acid residues, including two invariant histidine residues, His369 and His327, presumably involved in substrate binding and catalysis (7). Upon reduction, the sixth d_1 heme ligand (a hydroxide ion) is dissociated and the site becomes five-coordinated and able to bind the physiological substrate, as well as other small ligands.

Recently, two site-directed mutants of *Pa* cd_1 NiR (namely H327A and H369A), have been prepared by mutating the invariant histidines (His327 and His369) to alanines (9, 10). The 3D structure of both mutants shows in the distal d_1 heme pocket the substitution of Ala for His and the disappearance of Tyr10 along with the N-terminal arm; these local changes are associated to a large conformational reorganization involving a relocation of the c heme domain relative to the d_1 heme

Abbreviations used: *Pa* cd_1 NiR, *Pseudomonas aeruginosa* cd_1 nitrite reductase; *Pp* cd_1 NiR, *Paracoccus pantotrophus* cd_1 nitrite reductase; H369A, His369 to Ala; wt, wild type.

[1] These authors contributed equally to this work.

[2] To whom correspondence and reprint requests should be addressed at Dipartimento di Scienze Biochimiche "A. Rossi Fanelli," Università di Roma "La Sapienza," Piazzale Aldo Moro 5, 00185 Rome, Italy. Fax: +39-06-4440062. E-mail: f.cutruzzola@caspur.it.

0006-291X/02 $35.00

domain. Both mutants have lost their nitrite reductase activity, but still maintain the ability to reduce O_2 to water. Transient kinetics showed that the two histidines play different roles in catalysis, His369 being essential for the stabilization of the Michaelis complex with NO_2^- bound at the reduced d_1 heme iron (9).

It is well known that ferrous heme proteins generally display an affinity toward anionic ligands much lower than that of their ferric counterparts (11). Interestingly, reduced cd_1 NiR has an unusually high affinity for negatively charged ligands such as NO_2^-, the physiological substrate, and cyanide (12). The three-dimensional structure of the cyanide bound derivative of reduced cd_1 NiR from *Paracoccus pantotrophus* (13), suggests that the positive charge carried by the two invariant His might be essential for ligand stabilization. Therefore, we have studied the reaction of cyanide with the mutant H369A of *Pa* cd_1 NiR, together with that of the wild-type enzyme. In parallel, the crystal structure of reduced wt *Pa* cd_1 NiR saturated with cyanide has also been determined.

EXPERIMENTAL PROCEDURES

Mutagenesis and protein purification. Mutagenesis, subcloning, expression in *Pseudomonas putida*, and purification were carried out as described (9, 14, 15). The recombinant "semiapo"-protein was reconstituted with the d_1 heme extracted from *Pa* cd_1 NiR, as detailed in Ref. (14). *Pa* cd_1 NiR was purified following Parr *et al.* (16).

Static titrations. Cyanide binding to the reduced proteins (wild-type *Pa* cd_1 NiR and mutant H369A) was monitored spectrophotometrically under anaerobic conditions in 0.1 M potassium phosphate, pH 7.0 at 20°C. Optical spectra were recorded using a JASCO V570 or HP 8453 spectrophotometer. Protein samples (4–5 μM) were reduced with sodium ascorbate (10 mM) in a tonometer under positive nitrogen pressure. Following complete reduction, the protein was transferred into a cuvette sealed with a septum and sodium cyanide added anaerobically. The increase in absorbance at 625 nm for the wild-type protein or 632 nm for the mutant H369A was used to follow cyanide binding.

Stopped-flow experiments. Experiments were carried out anaerobically with a rapid mixing instrument equipped with a diode-array or a monochromator (DX.17MV, Applied Photophysics, Leatherhead, UK). The instrument uses a 150-W Xenon lamp, has a light path of 1 cm and in the diode-array mode can acquire up to 500 spectra with an acquisition time of 2.5 ms per spectrum. Curve fitting was performed with the software MATLAB (Math Works) and analysis of time-resolved spectra with the singular value decomposition (SVD) algorithm (17). All experiments were run in the presence of 10 mM glucose and catalytic amounts of glucose oxidase under N_2. Fully reduced cd_1 NiR (3–6 μM before mixing) was mixed with different sodium cyanide concentrations (0.10–10 mM for the mutant H369A and 0.05–0.5 mM for the wild-type NiR) in the presence of 10 mM ascorbate at 20°C. In the single wavelength acquisition mode, the reaction was followed at 625 nm for the wild type or 632 nm for the mutant H369A.

Crystallization of reduced cyanide-bound wild-type Pa cd_1 NiR. Orthorhombic crystals ($P2_12_12$) with cell dimensions (163.2 × 90.4 × 112.0 Å) were obtained in the presence of 2 M Na^+/K^+ phosphate in 50 mM Tris/HCl, pH 8.4, as previously described (6). The complex with cyanide was obtained by soaking (20 min at room temperature) oxidized crystals in a mother liquor containing 100 mM ascorbate and 60 mM KCN, pH 8.0, saturated with argon. The reduced cyanide-bound crystals were then soaked for a few seconds in a mother liquor containing 20% glycerol and cryocooled at 100 K using an Oxford cryosystem.

Data collection and structure refinement. Diffraction data on the orthorhombic crystals were collected at 100 K on beamline X11 at the DESY synchrotron (Hamburg) at 2.7 Å resolution on a MAR image-plate. Data were processed using DENZO (18) and scaled/merged by SCALA/TRUNCATE (19). The structure was solved by molecular replacement with AmoRe (20) using data between 10 and 3.5 Å and the reduced wild-type structure (7) as a search model. Refinement was performed with CNS (21) and graphical remodeling with TURBO-FRODO (22). The presence of a molecule of cyanide at the d_1 heme active site in both subunits was clearly indicated by strong Fourier difference (~8 sigma) and the position of the bound ligand was optimized. No Fourier difference was observed in the vicinity of the c heme and no significant conformational differences were observed elsewhere in the model. Water molecules were then placed automatically and checked manually. The final R factor was 21.0% (R_{free} = 24.7%) and includes residues from Asp3 to Tyr543 in subunit A and from Lys6 to Tyr543 in subunit B, 606 water molecules, one c heme, one d_1 heme and one cyanide molecule per subunit. The final refinement statistics are given in Table 1. The stereochemistry was analyzed by PROCHECK (23); 87% of residues were found to lie in most favorable regions of the Ramachandran plot, 11% in additionally allowed regions, 2% were found in generously allowed regions.

RESULTS

Static Titrations

Addition of cyanide to the reduced H369A mutant is associated with significant changes of the absorption bands characteristic of the d_1 heme (460 and 650 nm) (Fig. 1); in particular, absorbance at 632 nm increases with cyanide concentration. In contrast, no obvious changes are observed at the absorption bands characteristic of the c heme (520 and 550 nm). Therefore, cyanide binds only to the d_1 heme of the fully reduced protein, and the presence of isobestic points throughout the titration indicates that only two species are populated. Cyanide binding to the reduced wild-type *Pa* cd_1 NiR (12), reinvestigated in parallel, is associated to a peak centered at 625 nm (Fig. 1B).

The results show that H369A exhibits an affinity for cyanide lower than the wt enzyme; the dissociation constants (K_d) are 123 ± 12 μM for the mutant H369A, and 9.5 ± 0.6 μM for the wt protein. The Hill coefficient (1.37 ± 0.09 for the wt and 1.53 ± 0.16 for H369A, insets in Fig. 1), is essentially the same but for the wt protein it is considerably smaller than that previously reported (12).

Stopped-Flow Experiments

Figure 2 shows a set of the difference spectra recorded between 2.5 ms and a few seconds after mixing the reduced protein with cyanide; the time course at a single cyanide concentration (50 μM for the wt and 1 mM for the mutant) is given in the same figure.

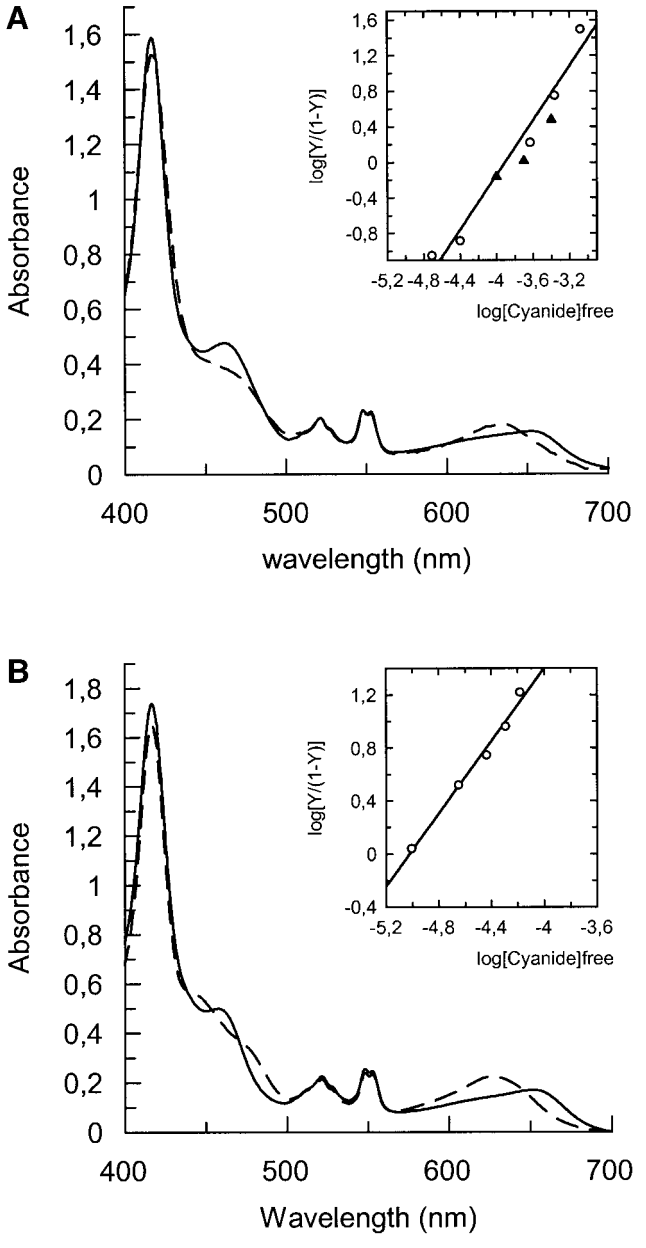

FIG. 1. Titration of fully reduced *Pa* cd_1 NiR with cyanide. Only two optical spectra, representing the initial and final species, are shown for clarity. (A) Mutant H369A (4.5 μM) and (B) wild-type NiR (4.9 μM) in the absence (continuous line) and presence (dashed line) of cyanide (1 mM cyanide in A and 0.1 mM in B). Titration in 0.1 M phosphate buffer, pH 7.0, at 20°C; the insets show the Hill plot (open circles), where Y is the fractional saturation of the protein with the ligand and $[cyanide]_{free}$ is the concentration of unbound ligand. For mutant H369A, binding data derived from kinetic measurements (black triangles) are also reported.

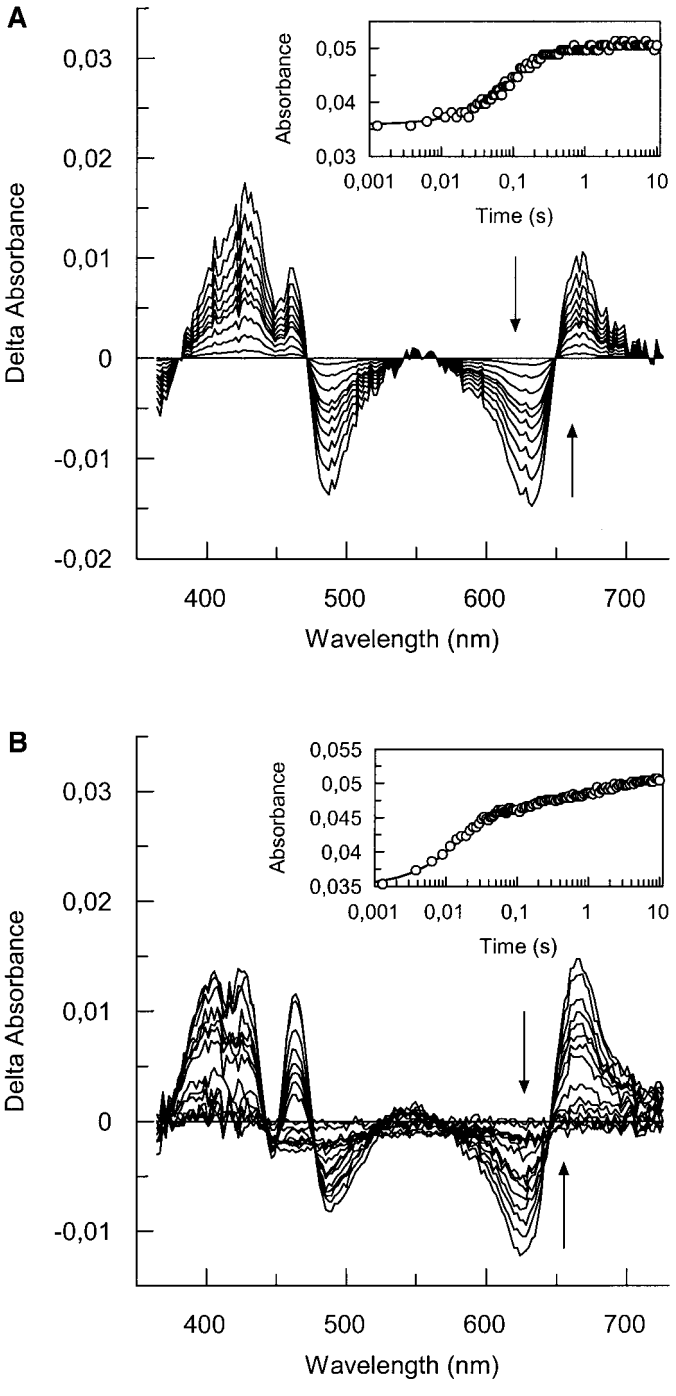

FIG. 2. Kinetic difference spectra observed after mixing the fully reduced cd_1 NiR with cyanide anaerobically. (A) 1.2 μM H369A + 1 mM cyanide; (B) 1.4 μM wt NiR + 50 μM cyanide (concentrations after mixing). The arrows indicate the direction of the time evolution, from 2.5 to 300 ms, of a selected number of spectra out of 80 acquired. The inset shows the time course at the maximum absorbance of the cyanide complex (632 nm for mutant H369A and 625 nm for wt NiR), fitted with a single exponential for the mutant, and with two exponentials for the wt protein (continuous line). Experiments carried out in 0.1 M phosphate buffer, pH 7.0 and 20°C.

For H369A, the first spectrum (2.5 ms) recorded after mixing the reduced protein with 1.0 mM cyanide shows that a large fraction of the unliganded reduced form is still present (Fig. 2A); the initial species evolves in a monophasic process to yield the reduced, cyanide-

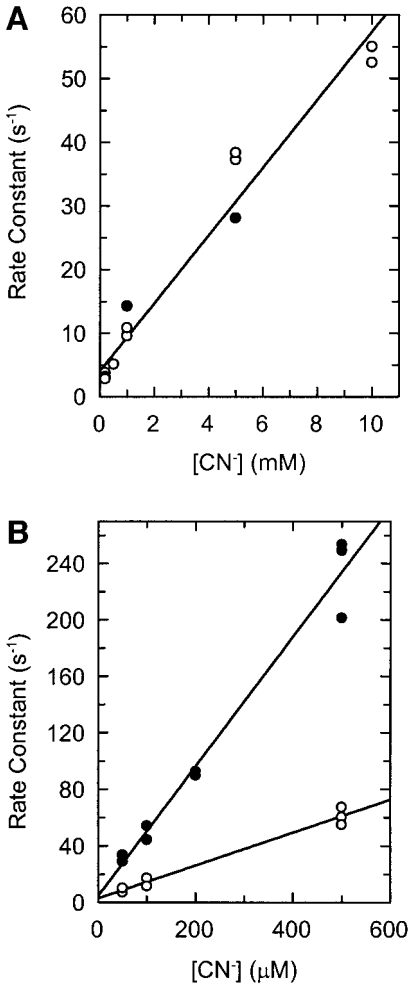

FIG. 3. The dependence of observed pseudo-first-order rate constant on cyanide concentration. (A) H369A: open circles represent data points obtained following the kinetics at single wavelength (632 nm) and black circles, data obtained from the acquisition of the whole spectral range (diode array mode). (B) wt NiR: black circles, k_1; open circles, k_2. Other conditions as in Fig. 2.

bound complex. The absorbance changes at the c heme bands (520 and 550 nm) are negligible, confirming that reduced c heme is unreactive toward cyanide. The apparent rate constant is cyanide concentration dependent (Fig. 3A), yielding a second-order rate constant of $k_1 = (5.3 \pm 0.3) \times 10^3\ M^{-1}\ s^{-1}$ for the reduced H369A. The amplitudes from the kinetic data agree well with those obtained in the static titrations (Fig. 1A, inset), indicating the self-consistency of these experiments.

In the case of wild-type *Pa* cd_1 NiR, the starting spectrum (the cyanide-free reduced species) quickly evolves to produce the cyanide-bound species through a complex process (Fig. 2B), which can be fitted to two exponentials. These two processes have variable amplitudes (the relative fraction of the slower phase increases as the cyanide concentration decreases), and both exhibit a linear dependence on cyanide concentration (Fig. 3B). The two second-order rate constants, $k_1 = (4.6 \pm 0.3) \times 10^5\ M^{-1}\ s^{-1}$ and $k_2 = (1.2 \pm 0.08) \times 10^5\ M^{-1}\ s^{-1}$, are comparable to those previously published (12). It is clear that the mutation H369A has a very large effect on the combination rate constant with cyanide (~100-fold decrease) and a smaller one on the affinity (~13-fold reduction), compared to the wt enzyme.

Structure of the Reduced Cyanide-Bound Pa cd_1 NiR

The overall three-dimensional structure of the reduced *Pa* cd_1 NiR saturated with cyanide determined to 2.7 Å is very similar to that of the reduced protein bound to NO (7): an rmsd of 0.2 Å is obtained upon superposition of the dimer's 1078 Cα atoms of the two structures. The two monomers in the dimer, related by a 2-fold noncrystallographic axis, superpose very well with a rmsd of 0.14 Å over 539 Cα atoms. As in the case of the oxidized and the reduced NO-complex, the B-factors are relatively high (Table 1).

A single peak of difference electron density was clearly visible at the d_1 heme site in a position closely similar in the two monomers; a cyanide anion could easily be fitted in this density with the Fe-C bond length of 1.83 Å and an Fe-C-N angle of 168° (Fig. 4). The weak deviation from linearity of the Fe-C-N angle in *Pa* cd_1 NiR may be taken as an indication of a strong Fe-CN^- bond (24). It is worthwhile noting that, within the error limits, the distances are identical for each ligand in the two subunits of *Pa* cd_1 NiR.

TABLE 1

Structural Statistics of Reduced *Pa* cd_1 NiR Bound to Cyanide

Data collection	
Space group	$P2_12_12$
Resolution[a] (Å)	2.7
R_{sym}[b] (%)	9.5 (35.6)[c]
$I/\sigma I$ (%)	6.3 (2.1)
Completeness (%)	90.3 (89.3)
Redundancy	2.2
Refinement	
Resolution (Å)	18–2.7
Total reflections	42035
R_{work}/R_{free}[d] (%)	20.4/24.7
Total atoms/AU (protein/water)	8627/605
Mean B-factor (Å): main/(side + solvent)	31.5/34.7
Rmsd B-factor (Å): main/side	1.7/3.2
Rmsd bonds (Å)	0.012
Rmsd angles, dihedrals, impropers (°)	1.9/25.7/1.71

[a] High-resolution cutoff criteria are $R_{sym} \approx 35\%$ and $I/\sigma I \approx 2$ in the outer resolution shell.

[b] $R_{sym} = \Sigma|I - \langle I\rangle|/\Sigma\langle I\rangle$, where I is intensity and $\langle I\rangle$ is the average I for all equivalent reflections.

[c] Values in parentheses are for the outer resolution shell.

[d] Number of reflections in the random test set is 1264 (3%).

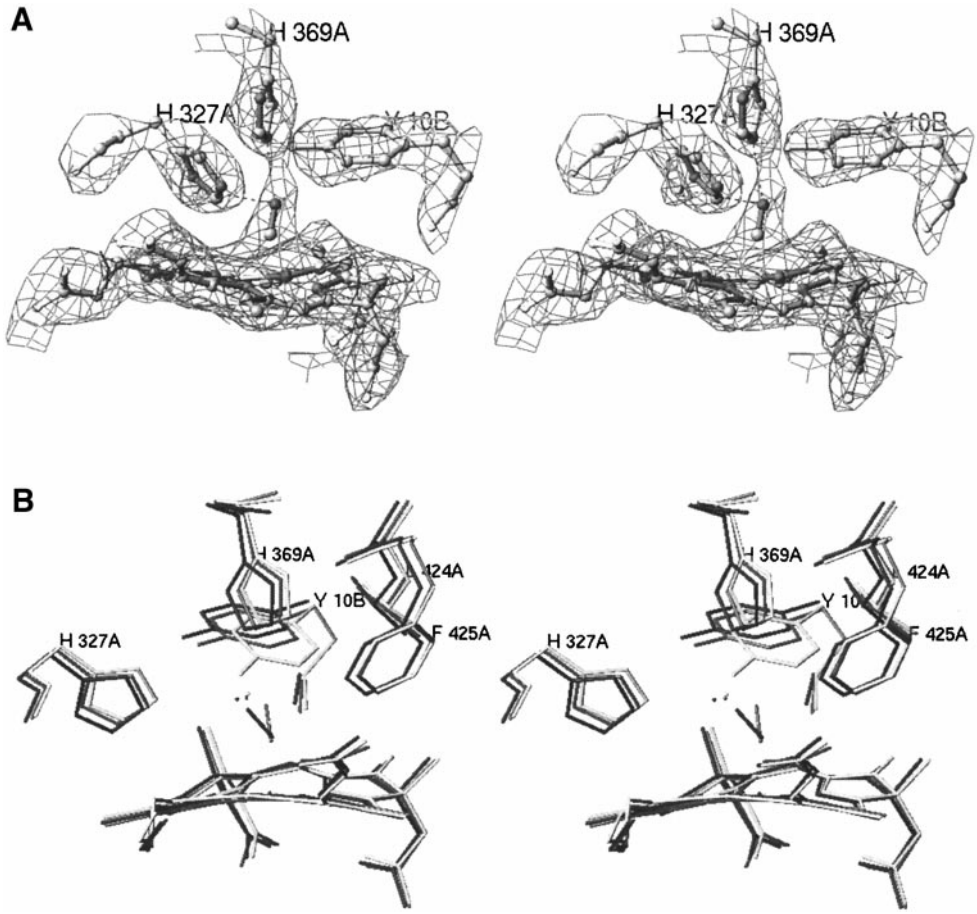

FIG. 4. Stereo view of the d1 heme active site of the subunit A of reduced wild-type NiR from *Pseudomonas aeruginosa*. (A) reduced NiR saturated with cyanide. The amino acid residues and the heme are represented in ball-and-stick. The $2F_o$-F_c electron density is contoured at 1 σ. (B) comparison of three derivatives of *Pa* cd1 NiR: reduced saturated with cyanide (dark gray) (PDB No. 1GJQ), reduced NO-bound (black) (PDB No. 1NNO) and oxidized (light gray) (PDB No. 1NIR). The models are represented in stick.

Among the residues of the d_1 heme pocket, only His369 is at a distance suitable for H-bond formation (apart from a water molecule conserved in all structures). His327 and Tyr10 are more than 3.5 Å away from the nitrogen atom of the cyanide, and thus are unlikely to be involved directly in the stabilization of the bound anion.

DISCUSSION

Previous stopped-flow investigations have shown a marked decrease in the affinity for nitrite in H369A (9). To demonstrate that the active site His369 is involved in the stabilization of other anionic ligands, we have investigated cyanide binding to *Pa* cd_1 NiR, comparing the mutant H369A with the wt enzyme. Since cyanide is not a substrate but just a ligand, it may be useful as a probe of the affinity of the ferrous d_1 heme for anions and the role of the structure of the protein in controlling binding. The results in this work clearly show that the affinity of the mutant H369A for cyanide is reduced (ca. 10-fold) compared to the wild-type protein.

Both wt NiR and mutant H369A are dimers in solution, as determined by gel filtration chromatography. The Hill coefficient ($n \sim 1.5$), observed in the cyanide binding to H369A and wt NiR, indicates a significant positive cooperativity between the two d_1 hemes, consistent with the dimeric structure of the enzyme. The molecular mechanism underlying cooperativity in the binding of cyanide is still unclear and will require further investigation. It is of interest however that a positive cooperativity between the two d_1 hemes has been reported in redox titrations of *Pa* cd_1 NiR (25) and in the binding of reduced *Pa* cd_1 NiR with other ligands, such as carbon monoxide (26) and metabisulfite (27). In contrast, cyanide binding to reduced cd_1 NiR from *Paracoccus pantotrophus* is characterized by a Hill coefficient of 0.85 associated with a higher affinity toward cyanide ($K_d \sim 1$ μM) (13).

It was previously shown that the d_1 heme pocket of mutant H369A is more open due to the replacement of His with Ala (9, 10); in principle this should facilitate ligand association by reducing the steric hindrance, as observed for CO binding to H369A by laser photolysis experiments (W. S., M.A., A. Bellelli, A. Arcovito, M.B., and F.C., unpublished work). In contrast, the second-order rate constant for cyanide binding to H369A ($k = 5.3 \times 10^3\ M^{-1}\ s^{-1}$) was found to be much smaller than either one of the two constants determined for wt NiR ($k_1 = 4.6 \times 10^5\ M^{-1}\ s^{-1}$ and $k_2 = 1.2 \times 10^5\ M^{-1}\ s^{-1}$). We conclude that reduced steric crowding of the distal site cannot be an explanation for the decreased cyanide binding to H369A.

At neutral pH cyanide is fully in the acid form ($pK_a \sim 9.5$). Based on the extensive experiments carried on monomeric hemeproteins, Mintorovitch *et al.* (28) reported that deprotonation of HCN in the active site may be the major kinetic barrier to cyanide binding. This mechanism involves diffusion of the neutral form (HCN) into the distal pocket followed by rapid combination of CN^- with the heme iron and proton donation to the imidazole of the distal histidine [which in sperm whale myoglobin is at position His64(E7)]. A decrease in the rate constant for complex formation with cyanide was indeed observed when the proton accepting side-chain His64(E7) was replaced by Ala in sperm whale metmyoglobin (29, 30). Based on our kinetic data, we propose that a similar role in controlling cyanide combination may by played by the distal histidine (His369), given that its imidazole is within H-bonding distance from the bound cyanide (Fig. 4). It is also known that for the cyanide complex of ferrous myoglobin, protonation of the ligand is a key step in the kinetics of cyanide dissociation (31). For example, for ferrous *Aplysia* myoglobin (which lacks the distal histidine), the rate constant for cyanide dissociation was found to be $0.02\ s^{-1}$ (32), significantly lower than the values reported for myoglobins containing His64(E7). Ignoring complexities arising from d_1 heme-heme interactions ($n \sim 1.5$), the dissociation rate constant of cyanide may be estimated to be $0.64\ s^{-1}$ for H369A and $4.35\ s^{-1}$ for the wt protein. Along the same lines, the decrease in the dissociation rate constant of cyanide calculated for mutant H369A suggests that also for the ferrous d_1 heme iron of *Pa* cd_1 NiR a protonation step might be involved in the rate determining step.

These mechanistic considerations are supported by examination of the structure of the reduced NO-bound derivative of H369A (10). In spite of the medium resolution, the position and H-bond network of NO in this mutant provide clear evidence for reduction of the electrostatic potential of the active site associated to the mutation, and thereby for a unique role of His369 in binding anions (10).

We conclude that the dominant factors regulating the affinity of anionic ligands (such as cyanide and nitrite) for reduced *Pa* cd_1 NiR appear to be H-bonding to the bound ligand by the distal amino acid residue(s), which facilitate charge transfer and (eventually) reductive cleavage, together with an overall positive electrostatic potential of the distal site and of the surroundings of the d_1 heme, which could contribute to ligand stabilization by counterbalancing the relatively weak intrinsic affinity of the ferrous heme iron for anionic ligands.

ACKNOWLEDGMENTS

W. Sun expresses his thanks to the International Center for Genetic Engineering and Biotechnology (ICGEB, Trieste, Italy) for the award of a postdoctoral fellowship. A. Giuffrè (Rome, Italy) is gratefully acknowledged for the help in the calculation of kinetic experiments. Grants from the Consiglio Nazionale delle Ricerche of Italy (Target Project on Biotechnology), Ministero dell'Università of Italy (Progetto di Ricerca di Interesse Nazionale 2001, "Dinamica Strutturale di Metalloproteine"), are gratefully acknowledged.

REFERENCES

1. Averill, B. A. (1996) Dissimilatory nitrite and nitric oxide reductases. *Chem. Rev.* **96,** 2951–2964.
2. Zumft, W. G. (1997) Cell biology and molecular basis of denitrification. *Microbiol. Mol. Biol. Rev.* **61,** 533–616.
3. Cutruzzolà, F. (1999) Bacterial nitric oxide synthesis. *Biochim. Biophys. Acta* **1411,** 231–249.
4. Horio, T., Higashi, T., Sasagawa, M., Kusai, K., Nakai, M., and Okunuki, K. (1960) Purification and properties of cytochrome oxidase from *Pseudomonas aeruginosa. Biochem. J.* **77,** 194–201.
5. Yamanaka, T., Ota, A., and Okunuki, K. (1961) A nitrite reducing system reconstructed with purified cytochrome components of *Pseudomonas aeruginosa. Biochim. Biophys. Acta* **53,** 294–308.
6. Nurizzo, D., Silvestrini, M. C., Mathieu, M., Cutruzzolà, F., Bourgeois, D., Fulop, V., Hajdu, J., Brunori, M., Tegoni, M., and Cambillau, C. (1997) N-terminal arm exchange is observed in the 2.15 Å crystal structure of oxidized nitrite reductase from *Pseudomonas aeruginosa. Structure (London)* **5,** 1157–1171.
7. Nurizzo, D., Cutruzzolà, F., Arese, M., Bourgeois, D., Brunori, M., Tegoni, M., and Cambillau, C. (1998) Conformational changes occurring upon reduction and NO binding in nitrite reductase from *Pseudomonas aeruginosa. Biochemistry* **37,** 13987–13996.
8. Nurizzo, D., Cutruzzolà, F., Arese, M., Bourgeois, D., Brunori, M., Cambillau, C., and Tegoni, M. (1999) Does the reduction of c heme trigger the conformational change of crystalline nitrite reductase? *J. Biol. Chem.* **274,** 14997–15004.
9. Cutruzzolà, F., Brown, K., Wilson, E. K., Bellelli, A., Arese, M., Tegoni, M., Cambillau, C., and Brunori, M. (2001) The nitrite reductase from *Pseudomonas aeruginosa:* Essential role of two active-site histidines in the catalytic and structural properties. *Proc. Natl. Acad. Sci. USA* **98,** 2232–2237.
10. Brown, K., Roig-Zamboni, V., Cutruzzolà, F., Arese, M., Sun, W., Brunori, M., Cambillau, C., and Tegoni, M. (2001) Domain swing upon His to Ala mutation in nitrite reductase of *Pseudomonas aeruginosa. J. Mol. Biol.,* **312,** 541–554.

11. Antonini, E., and Brunori, M. (1971) Hemoglobin and Myoglobin in Their Reactions with Ligands, North-Holland, Amsterdam.
12. Barber, D., Parr, S. R., and Greenwood, C. (1978) The reactions of *Pseudomonas* cytochrome *c*-551 oxidase with potassium cyanide. *Biochem. J.* **175,** 239–249.
13. Jafferji, A., Allen, J. W. A., Ferguson, S. J., and Fulop, V. (2000) X-ray crystallographic study of cyanide binding provides insights into the structure–function relationship for cytochrome cd_1 nitrite reductase from *Paracoccus pantotrophus*. *J. Biol. Chem.* **275,** 25089–25094.
14. Silvestrini, M. C., Cutruzzolà, F., D'Alessandro, R., Brunori, M., Fochesato, N., and Zennaro, E. (1992) Expression of *Pseudomonas aeruginosa* nitrite reductase in *Pseudomonas putida* and characterization of the recombinant protein. *Biochem. J.* **285,** 661–666.
15. Cutruzzolà, F., Arese, M., Grasso, S., Bellelli, A., and Brunori, M. (1997) Mutagenesis of nitrite reductase from *Pseudomonas aeruginosa:* Tyrosine 10 is not involved in catalysis. *FEBS Lett.* **412,** 365–369.
16. Parr, S. R., Barber, D., Greenwood, C., Phillips, B. W., and Melling, J. (1976) A purification procedure for the soluble cytochrome oxidase and some other respiratory proteins from *Pseudomonas aeruginosa*. *Biochem. J.* **157,** 423–430.
17. Henry, E. R., and Hofrichter, J. (1992) Singular value decomposition: Application to analysis of experimental data. *Methods Enzymol.* **210,** 129–192.
18. Otwinowski, Z., and Minor, W. (1997) Processing of X-ray diffraction data collected in oscillation mode. *Methods Enzymol.* **276,** 307–326.
19. CCP4 (1994) The CCP4 suite: Programs for crystallography. *Acta Cryst.* **D50,** 760–766.
20. Navaza, J. (1994) AmoRe: An automated package for molecular replacement. *Acta Cryst.* **A50,** 157–163.
21. Brunger, A. T., Adams, P. D., Clore, G. M., DeLano, W. L., Gros, P., Grosse-Kunstleve, R. W., Jiang, J. S., Kuszewski, J., Nilges, M., Pannu, N. S., Read, R. J., Rice, L. M., Simonson, T., and Warren, G. L. (1998) Crystallography & NMR system: A new software suite for macromolecular structure determination. *Acta Cryst.* **D54,** 905–921.
22. Roussel, A., and Cambillau, C. (1991) TURBO-FRODO Graphics Package (Graphics, S., Ed.), Silicon Graphics Geometry Partners Directory, Mountain View, CA.
23. Laskowski, R. A., Rullmannn, J. A., MacArthur, M. W., Kaptein, R., and Thornton, J. M. (1996) AQUA and PROCHECK-NMR: Programs for checking the quality of protein structures solved by NMR. *J. Biomol. NMR* **8**(4), 477–486.
24. Yu, N. T. (1986) Resonance Raman studies of ligand binding. *Methods Enzymol.* **130,** 350–409.
25. Blatt, Y., and Pecht, I. (1979) Allosteric cooperative interactions among redox sites of *Pseudomonas* cytochrome oxidase. *Biochemistry* **18,** 2917–2922.
26. Parr, S. R., Wilson, W. T., and Greenwood, C. (1975) The reaction of *Pseudomonas aeruginosa* cytochrome *c* oxidase with carbon monoxide. *Biochem. J.* **151,** 51–59.
27. Parr, S. R., Wilson, W. T., and Greenwood, C. (1974) The reaction of *Pseudomonas aeurginosa* cytochrome *c* oxidase with sodium metabisulphite. *Biochem. J.* **139,** 273–276.
28. Mintorovitch, J., van Pelt, D., and Satterlee, J. D. (1989) Kinetic study of the slow cyanide binding to *Glycera dibranchiata* monomer hemoglobin components III and IV. *Biochemistry* **28,** 6099–6104.
29. Brancaccio, A., Cutruzzolà, F., Travaglini Allocatelli, C., Brunori, M., Smerdon, S. J., Wilkinson, A. J., Dou, Y., Keenan, D., Ikeda-Saito, M., Brantley, R. E., and Olson, J. S. (1994) Structural factors governing azide and cyanide binding to mammalian metmyoglobins. *J. Biol. Chem.* **269,** 13843–13853.
30. Dou, Y., Olson, J. S., Wilkinson, A. J., and Ikeda-Saito, M. (1996) Mechanism of hydrogen cyanide binding to myoglobin. *Biochemistry* **35,** 7107–7113.
31. Travaglini Allocatelli, C., Cutruzzolà, F., Brancaccio, A., Brunori, M., Qin, J., and La Mar, G. N. (1993) Structural and functional characterization of sperm whale myoglobin mutants: Role of arginine (E10) in ligand stabilization. *Biochemistry* **32,** 6041–6049.
32. Bellelli, A., Antonini, G., Brunori, M., Springer, B. A., and Sligar, S. G. (1990) Transient spectroscopy of the reaction of cyanide with ferrous myoglobin. Effect of distal side residues. *J. Biol. Chem.* **265,** 18898–18901.